

Potential-pH diagrams for complex systems

JOHN C. ANGUS, BEI LU, MICHAEL J. ZAPPIA

Department of Chemical Engineering, Case Western Reserve University, Cleveland, Ohio 44106, USA

Received 19 February 1986

A generalized thermodynamic analysis and a geometric interpretation of potential-pH diagrams for multi-element systems are presented. The presence of reactive gases, e.g. CO₂ and SO₂, and complex-forming species, e.g. NH₃ and Cl⁻, are expressly considered. The equilibrium state is described by a set of independent formation reactions of all species containing the active redox element, M. The formation reactions are written in terms of a user-specified set of primitive species, e.g. M, H₂O, H⁺, e, X and Y, where X and Y could be CO₂ and Cl⁻ for example. Some of these primitive species, e.g. M and e, may be virtual species, that is, they do not have an independent existence as separate entities in the reaction mixture. This procedure permits an explicit algebraic solution for the potential-pH diagram. Examples of Pourbaix and predominance diagrams for complex uranium and chromium systems are given.

Nomenclature	w_i	stoichiometric coefficient for H ₂ O in generalized formation reaction
A	defined by Equation 41	[X]
a	activity	x_i
a_M	overall activity of redox element M	
D	maximum dimensionality of diagram	y_i
E	electrochemical potential	
F	Faraday's constant	z_i
f	degrees of freedom	
$\Delta G_{f,n}^0$	standard free energy of formation of species n	α_i
h_i	stoichiometric coefficient for H ⁺ in generalized formation reaction	
M	symbol for redox element	γ
M_i	symbol for i th species containing redox element M	μ
[M_i]	molal concentration of species M_i	v_i
[M] _T	total dissolved concentration of redox element M	
n	number of species containing redox element M	<i>Subscripts</i>
P	number of phases	aq
P_j	symbol for primitive species	b, c, d
p	pressure	
p_{ij}	stoichiometric coefficient for species P_j in generalized formation reaction	i
r	number of independent reactions	
R	gas constant	j
s	number of species	M
t	number of primitive species	s, t, u, v
		<i>Superscripts</i>
		o
		r

1. Introduction

Potential–pH diagrams have long been used to describe phase stability in aqueous redox systems [1–4]. They have found widespread use in corrosion studies, geochemistry and hydrometallurgy. In recent years, significant work has been expended in the construction of potential–pH diagrams by computer [5–17]. These efforts require a systematization of the chemical thermodynamic theory underlying the diagrams and a clear idea of the assumptions necessary to perform the computations.

A thermodynamic framework and computational method for constructing potential–pH diagrams have recently been presented by one of the authors [17]. That work was, however, restricted to the relatively simple case in which the system is comprised only of the redox element, M , plus hydrogen and oxygen. In the present paper we generalize the methods to include other elements that may be present, for example, in reactive gases, e.g. SO_2 and CO_2 , and complex-forming dissolved species, e.g. NH_3 and Cl^- .

First, a general thermodynamic analysis and geometric interpretation of potential–pH diagrams are presented. Second, computational methods are discussed and rigorous algebraic solutions are presented for systems containing additional elements. Third, examples of several multi-element computer-generated potential–pH diagrams are given.

2. Discussion of prior work

For the three-element (M – H – O) system, the Pourbaix diagram is a three-dimensional surface in chemical potential space [17]. The three axes are the chemical potentials of the electrons, the protons and the redox element, M . By convention, practical measures of these chemical potentials are used, i.e. the electrode potential, E , the pH and the logarithm of the activity, a_M , of the redox element, M . Also, by convention, the two-dimensional projection on the E –pH plane of the three-dimensional figure is normally reported.

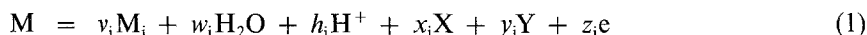
Because the analysis in [17] was restricted to simple three-element systems, the influence of reactive counter ions, e.g. Cl^- , and reactive gas phases, e.g. CO_2 , was ignored. All counter ions were assumed to be totally inert and the gas phase, if present, was tacitly assumed to contain only inert gases and the equilibrium partial pressures of H_2 and O_2 , fixed by the prevailing pH and potential. These restrictions, while widely employed, exclude many situations of great practical importance.

3. Thermodynamic analysis

3.1. Chemical reaction equilibrium

In choosing a set of independent reactions, it is essential that no *a priori* assumptions about ‘dominant’ reactions or ‘major’ species be made that limit the generality of the results. Furthermore, for computational simplicity and generality the reaction scheme should permit the addition or deletion of species without changing the mathematical structure of the solution.

The set of independent reactions is generated by writing $(n - 1)$ formation reactions for the n species containing the active redox element, M . The formation reactions are written using the primitive species M , H^+ , H_2O , X , Y and e . The formation reactions for M_i are written in the following standard form:



For example, consider the formation reaction for FeCO_3 :



where the following assignments are made: $M = \text{Fe}$, $M_i = \text{FeCO}_3$, $X = \text{CO}_2$; $v_i = +1$, $w_i = -1$, $h_i = +2$, $x_i = -1$, $y_i = 0$ and $z_i = +2$.

Writing the formation reactions in this form has several advantages, e.g. the resulting equilibrium equations are particularly well suited for determining phase stability (see Section 3.6) and the set of equilibrium equations can be solved sequentially rather than simultaneously upon specification of the appropriate activities (see Sections 4.1.1 and 4.2). Furthermore, writing all equations per atom of M gives the stoichiometric coefficients a simple meaning, e.g. the stoichiometric coefficient, z_i , for the electrons is equal to the electrochemical valence of element M in species M_i .

3.2. Primitive species

There is an element of arbitrariness in the choice of primitive species. For example, for systems containing carbonates one could choose either CO_2 gas, H_2CO_3 or the CO_3^{2-} or HCO_3^- ions. If CO_2 gas pressure is being controlled then CO_2 gas is the obvious choice. If the CO_3^{2-} concentration is controlled then CO_3^{2-} is the logical primitive species. For systems in complete chemical equilibrium, i.e. gaseous systems at very high temperatures, the most useful choice of primitive species is often the elements themselves. For example, for very high temperature hydrocarbon gases, a set of independent reactions can be written by writing formation reactions for all compounds, molecular fragments and ions from elemental carbon, hydrogen and electrons. The general procedure of writing a set of independent reactions by writing formation reactions from primitive species is not new and has been used by Brinkley [18] and discussed by Denbigh [19] among others.

It would be tempting to conclude that the number of primitive species is always equal to the number of elements plus one for any system that contains charged species. This is, in fact, true for the high temperature gaseous system mentioned above when complete chemical equilibrium among all possible species is approached. However, at low temperature the persistence of functional groups as stable and metastable entities negates this simple rule. For example, an aqueous system containing copper in which the only reactive counter ions are CN^- would have five elements, Cu, H, O, C and N. Only five primitive species, Cu, H^+ , H_2O , CN^- and e , would be required to describe the complete reaction set.

It is clear that writing the set of independent reactions requires extrathermodynamic considerations and can only be performed with an understanding of the chemistry of the system of interest.

3.3. Virtual species

Not all of the primitive species need to exist physically as independent entities in the system. Even if they are not physically present, their chemical potentials can be well defined. Species of this type, which we call virtual species, are included to generalize the formalism and to simplify the computations. The most common example of this procedure is the separation of redox reactions into half cell reactions involving electrons. The free electrons do not exist as distinct entities with a measurable concentration in aqueous reaction mixtures, yet their chemical potential is well defined and measurable. The chemical potential of an element is also a well defined quantity even when it is not physically present as the free element in a reaction mixture. This has been pointed out by White [20] for gas phase systems and by Angus [17] for the aqueous redox systems of interest here.

3.4. Phase rule analysis

For chemically reacting systems the phase rule may be written

$$f = s - r - P + 2 \quad (3)$$

where s is the total number of species (both real and virtual), r is the number of independent

reactions that can be written among the real and virtual species and P is the number of phases.

We apply the phase rule to a system with n species containing M . In addition to M there are the other five primitive species, H_2O , H^+ , e , X and Y , which are needed to write the formation reactions. Substituting into Equation 3:

$$f = (n + 5) - (n - 1) - P + 2 \quad (4)$$

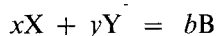
$$f = 8 - P \quad (5)$$

When both temperature and pressure are fixed, Equation 5 becomes

$$f = 6 - P \quad (6)$$

For systems comprised only of the elements, M , H and O , the primitive species X and Y are not necessary and Equation 6 reduces to $f = 4 - P$, the result given in [17].

It may happen that the primitive species react with one another. For example



or



In all of these cases there is one additional reaction and one additional species, e.g. B . Consequently the phase rule analysis remains unchanged, assuming B is not a solid phase. Also, as noted in [17], no provision is made to ensure electroneutrality. Again, this condition imposes one more equation and one more species, an inert counter ion, leaving the analysis the same.

Equations 4, 5 and 6 follow from the situation when the chemical reaction equilibria can be written using six primitive species as in Equation 1. These cover most situations of practical interest. However, if a more general formalism is required, one can simply generalize these results. For example, the general chemical reaction in standard form would be

$$M = v_i M_i + \sum_j^{t-2} p_{ij} P_j + z_i e \quad (7)$$

where P_j are the $(t - 2)$ primitive species required in addition to the electrons, e , and M . For fixed temperature and pressure the general form of the phase rule becomes

$$f = t - P \quad (8)$$

where t is the total number of primitive species required to describe the stoichiometry.

The key element in determining the number of independent variables is writing the independent chemical reactions in terms of appropriate primitive species. This cannot be done using thermodynamic theory alone and must involve a good understanding of the nature of the system in question. The phase rule provides the logical machinery to convert an essentially heuristic understanding of the system chemistry into a formal statement of the number of independent variables. In this sense the phase rule is not truly a predictive theory.

3.5. Dimensionality of diagrams

Potential–pH diagrams are a special type of a phase diagram in which each dimension is a chemical potential. Equation 8 specifies the number of chemical potentials that may be independently chosen and, hence, specifies the number of dimensions of the diagrams. Setting $P = 1$ (the minimum number of phases) gives the maximum number of dimensions, D , required to represent graphically the diagram.

$$D = t - 1 \quad (9)$$

For systems comprised solely of M , H and O , four primitive species are required to write the

chemical reactions: M, H⁺, H₂O and e. Therefore $t = 4$ and the chemical potential diagram is inherently three-dimensional. When six primitive species are required, the diagram is five-dimensional. In order to reduce it to three dimensions, the chemical potentials of two of the primitive species must be fixed at constant values.

3.6. Phase stability

Consider two solid species, M_u and M_v, in contact with the same aqueous phase. Initially assume that M_u and M_v are separately in equilibrium with the primitive species M, H⁺, H₂O, X, Y and e. Therefore, from Equation 1 one has two equilibrium relationships, one for solid M_u and one for solid M_v:

$$(\mu_M)_u = v_u \mu_u + w_u \mu_{H_2O} + h_u \mu_{H^+} + x_u \mu_X + y_u \mu_Y + z_u \mu_e \quad (10)$$

$$(\mu_M)_v = v_v \mu_v + w_v \mu_{H_2O} + h_v \mu_{H^+} + x_v \mu_X + y_v \mu_Y + z_v \mu_e \quad (11)$$

where $(\mu_M)_u$ and $(\mu_M)_v$ are the chemical potentials of M within solids M_u and M_v, respectively.

We consider the situation encountered both physically and computationally when the potential, the pH and the activities of both X and Y are held constant. However, for a three-phase system the phase rule (Equation 6) indicates that only three of these variables can be arbitrarily fixed. Since four chemical potentials have been specified, the system is overspecified and one of the solid phases must disappear. The stable solid phase can be determined by computing the overall free energy change, ΔG , for the transition between the phases. Writing Equation 1 for both M_u and M_v and eliminating the element M, one has

$$v_u M_u + w_u H_2O + h_u H^+ + x_u X + y_u Y + z_u e = v_v M_v + w_v H_2O + h_v H^+ + x_v X + y_v Y + z_v e \quad (12)$$

The free energy change for this reaction is

$$\begin{aligned} \Delta G = & v_v \mu_v - v_u \mu_u + (w_v - w_u) \mu_{H_2O} + (h_v - h_u) \mu_{H^+} \\ & + (x_v - x_u) \mu_X + (y_v - y_u) \mu_Y + (z_v - z_u) \mu_e \end{aligned} \quad (13)$$

However, using Equations 10 and 11, Equation 13 can be reduced to

$$\Delta G = (\mu_M)_v - (\mu_M)_u \quad (14)$$

Equation 14 shows that the free energy change for the transition between two solid phases is equal to the difference in the chemical potential of the redox element *within* the solid phases. When the two solids, M_u and M_v, are in equilibrium, $\Delta G = 0$ and therefore $(\mu_M)_u = (\mu_M)_v$. The chemical potential of any solid phase, M_s, can be computed directly from Equation 34. Therefore, Equation 14 provides an extraordinarily simple test for the stability of solid phases.

Furthermore, using Equation 33 the method can also be used to determine the stability of a solid with respect to an aqueous phase. In principle one can, of course, determine the stability of a solid phase by comparing the value of activity, a_s , of solid M_s with the activity of M_s in the solution. However, very often the solid species does not exist as such in the dissolved state. In these situations the chemical potential of active element is an easier criterion to apply.

4. Calculations of equilibrium composition

4.1. Summary of basic equations

4.1.1. Equations for species containing active element. The basic equilibrium criterion for reaction 1

is

$$\mu_M = v_i \mu_i + w_i \mu_{\text{H}_2\text{O}} + h_i \mu_{\text{H}^+} + x_i \mu_X + y_i \mu_Y + z_i \mu_e \quad (15)$$

If all of the chemical species are maintained in their standard states, Equation 15 becomes

$$\mu_M^0 = v_i \mu_i^0 + w_i \mu_{\text{H}_2\text{O}}^0 + h_i \mu_{\text{H}^+}^0 + x_i \mu_X^0 + y_i \mu_Y^0 + z_i \mu_e^0 \quad (16)$$

where the term μ_e^0 is the equilibrium chemical potential of electrons obtained when the chemical species in reaction 1 are held at their standard states. Subtracting Equation 16 from Equation 15 and rearranging gives:

$$\begin{aligned} v_i(\mu_i - \mu_i^0) &= (\mu_M - \mu_M^0) - w_i(\mu_{\text{H}_2\text{O}} - \mu_{\text{H}_2\text{O}}^0) - h_i(\mu_{\text{H}^+} - \mu_{\text{H}^+}^0) \\ &\quad - x_i(\mu_X - \mu_X^0) - y_i(\mu_Y - \mu_Y^0) - z_i(\mu_e - \mu_e^0) \end{aligned} \quad (17)$$

We are mainly interested in the activity, a_i , of M_i . The chemical potential and standard chemical potential of M_i are always related by a_i .

$$\mu_i = \mu_i^0 + RT \ln a_i \quad (18)$$

Combining Equations 17 and 18 and solving for $a_i^{v_i}$ one finds:

$$\begin{aligned} a_i^{v_i} &= \exp \left\{ \left(\frac{1}{RT} \right) [(\mu_M - \mu_M^0) - h_i(\mu_{\text{H}^+} - \mu_{\text{H}^+}^0) - w_i(\mu_{\text{H}_2\text{O}} - \mu_{\text{H}_2\text{O}}^0) \right. \\ &\quad \left. - x_i(\mu_X - \mu_X^0) - y_i(\mu_Y - \mu_Y^0) - z_i(\mu_e - \mu_e^0)] \right\} \end{aligned} \quad (19)$$

The generalized form of Equation 19 for an arbitrary number, t , of primitive species is clearly

$$a_i^{v_i} = \exp \left\{ \left(\frac{1}{RT} \right) \left[(\mu_M - \mu_M^0) - \sum_j^{t-2} p_{ij}(\mu_j - \mu_j^0) - z_i(\mu_e - \mu_e^0) \right] \right\} \quad (20)$$

Equations 19 and 20 give the activity of M_i in terms of the chemical potentials of the primitive species. They are the basic equilibrium equations upon which the calculations are based. Note that only differences in chemical potentials appear in Equations 19 and 20. Absolute values of chemical potential, which are not accessible, are not required.

4.1.2. Discussion of potential and free energy conventions. Here we discuss the conventions used to relate the theory to measurable quantities such as potential differences. The usual approach is to report the difference between the chemical potential of the electrons, μ_e , in equilibrium with reaction 1 and the chemical potential of electrons in equilibrium with a reference electrode. For the standard hydrogen electrode, $\text{H}^+ + e = \frac{1}{2}\text{H}_2$, the equilibrium expression is

$$\mu_{\text{H}^+}^0 + \mu_e^r = \frac{1}{2} \mu_{\text{H}_2}^0 \quad (21)$$

Combining Equations 16 and 21, one finds

$$-z_i(\mu_e^0 - \mu_e^r) = [v_i \mu_i^0 + w_i \mu_{\text{H}_2\text{O}}^0 + h_i \mu_{\text{H}^+}^0 + x_i \mu_X^0 + y_i \mu_Y^0 - \mu_M^0] + z_i(\mu_{\text{H}_2}^0/2 - \mu_{\text{H}^+}^0) \quad (22)$$

The convention used for relating μ_e to E , is

$$\mu_e = -FE \quad (23)$$

This convention differs only in sign from that proposed by Ramsey [21]. We choose the opposite sign convention to be consistent with virtually all other published potential–pH diagrams. Furthermore, it appears logically more consistent with simple qualitative arguments, i.e. high (positive) chemical potentials of electrons, which correspond to large ‘escaping tendency’ of electrons [22], should correspond to negative electric potentials.

From Equation 23 and Equation 22, one finds

$$E_i^0 - E^r = \frac{1}{z_i F} [v_i \mu_i^0 + w_i \mu_{\text{H}_2\text{O}}^0 + h_i \mu_{\text{H}^+}^0 + x_i \mu_{\text{X}}^0 + y_i \mu_{\text{Y}}^0 - \mu_{\text{M}}^0] + \frac{1}{F} (\mu_{\text{H}_2}^0/2 - \mu_{\text{H}^+}^0) \quad (24)$$

where $E_i^0 \equiv -\mu_i^0/F$ is called the standard electrode potential for the formation of species M_i by reaction 1. Furthermore, if the reference electrode is held at fixed unchanging conditions, the E^r , $\mu_{\text{H}_2}^0$ and $\mu_{\text{H}^+}^0$ are constant. For the standard hydrogen electrode it is customary to arbitrarily assign $E^r = 0$ and $(\mu_{\text{H}_2}^0/2 - \mu_{\text{H}^+}^0) = 0$, leaving

$$E_i^0 = \frac{1}{z_i F} [v_i \mu_i^0 + w_i \mu_{\text{H}_2\text{O}}^0 + h_i \mu_{\text{H}^+}^0 + x_i \mu_{\text{X}}^0 + y_i \mu_{\text{Y}}^0 - \mu_{\text{M}}^0] \quad (25)$$

This convention is permissible precisely because only differences in potential enter into normal thermochemical computations, i.e. absolute potentials are not required.

Equation 25 can be used with a self-consistent set of free energy of formation data ($\mu_n^0 = \Delta G_{f,n}^0$) to compute values of E_i^0 . This is the procedure used here to convert tabulated standard free energies of formation into standard potentials for use with our working equations.

Finally, note that the bracketed term on the right hand side of Equation 25 is the ΔG^0 for the half cell reaction 1 as conventionally defined, i.e. considering only chemical species. Therefore, with our conventions,

$$E_i^0 = \frac{\Delta G_i^0}{z_i F} \quad (26)$$

This convention is identical to that used in Pourbaix's Atlas [2].

4.1.3. Practical variables. The following conventions are used to relate the chemical potential differences of the other primitive species to practical variables:

$$\mu_{\text{H}} - \mu_{\text{H}^+}^0 = -2.30259RT(\text{pH}) \quad (27)$$

$$\mu_{\text{H}_2\text{O}} - \mu_{\text{H}_2\text{O}}^0 = RT \ln a_{\text{H}_2\text{O}} \quad (28)$$

$$\mu_{\text{X}} - \mu_{\text{X}}^0 = RT \ln a_{\text{X}} \quad (29)$$

$$\mu_{\text{Y}} - \mu_{\text{Y}}^0 = RT \ln a_{\text{Y}} \quad (30)$$

If primitive species, X, is a dissolved species, then $a_{\text{X}} = \gamma_{\text{X}}[\text{X}]$. If X is a gas, then $a_{\text{X}} = f_{\text{X}}$, where f_{X} is the fugacity of X and the standard state for X is chosen to be pure X in the ideal gas state at unity fugacity. If X is a pure solid, and this pure solid is chosen to be the standard state, then $a_{\text{X}} = 1$.

4.2. Summary of working equations

4.2.1. Assumptions. Equations 27–30 are rigorously correct under all circumstances. It is extremely convenient, however, to replace Equation 28 with

$$\mu_{\text{H}_2\text{O}} - \mu_{\text{H}_2\text{O}}^0 = 0 \quad (31)$$

Equation 31 is an assumption that is only approximately correct even at low concentrations. This assumption is implicit in many prior calculations of equilibria in aqueous systems and will be used here as well. It is often justifiable on the grounds that it introduces no greater error than the assumption of ideal solutions, which is also often made for lack of knowledge of activity coefficients. However, for accurate work it is necessary to include the activity of H_2O as a variable. Including $a_{\text{H}_2\text{O}}$ as a variable complicates the calculations and, in fact, forces one to perform an iterative numerical solution for each equilibrium composition rather than a sequential algebraic solution.

The chemical potentials of all of the real species including H_2O must be related through the Gibbs–Duhem equation. This relationship would normally be introduced through the functional form of the equation for the activity coefficients which, if correct, must obey the Gibbs–Duhem equation. It is this additional relationship, not explicitly used here, which is replaced by Equation 31.

4.2.2. General equilibrium equation in practical variables. The a_i can be determined in terms of practical variables by combining Equations 19, 23, 27, 29, 30 and 31.

$$a_i^{v_i} = \exp \left[\frac{\mu_M - \mu_M^0}{RT} + 2.30259h_i(\text{pH}) - x_i \ln a_X - y_i \ln a_Y + \frac{z_i F}{RT} (E - E_i^0) \right] \quad (32)$$

4.2.3. Equilibrium in aqueous phase. The chemical potential of M in the aqueous phase can be obtained exactly as in [17] by summing Equation 32 over all dissolved species and solving for $(\mu_M - \mu_M^0)/RT$.

$$\left[\frac{\mu_M - \mu_M^0}{RT} \right]_{\text{aq}} = -\ln \Sigma \exp \left[2.30259h_d(\text{pH}) - x_d \ln a_X - y_d \ln a_Y + \frac{z_d F}{RT} (E - E_d^0) \right] + \ln (\Sigma a_d^{v_d}) \quad (33)$$

The sums in Equation 33 are over the dissolved species, M_d . Equation 33 clearly shows that the chemical potential, μ_M , of M is well defined even when M does not exist as the free element in the aqueous phase.

4.2.4. Equilibrium between one solid and the aqueous phase. Here, only the case of a pure solid phase, M_s , for which the activity is unity is considered. Setting the left hand side of Equation 19 equal to one, using Equations 23, 27, 29, 30 and 31 and solving for $(\mu_M - \mu_M^0)/RT$, one finds

$$\left[\frac{\mu_M - \mu_M^0}{RT} \right]_s = -2.30259h_s(\text{pH}) + x_s \ln a_X + y_s \ln a_Y - \frac{z_s F}{RT} (E - E_s^0) \quad (34)$$

Equation 34 gives the chemical potential of M in the solid phase, M_s , as a function of pH, a_X , a_Y and E . Eliminating $(\mu_M - \mu_M^0)/RT$ between Equations 32 and 34, one obtains

$$a_d^{v_d} = \exp \left\{ 2.30259(h_d - h_s)(\text{pH}) - (x_d - x_s) \ln a_X - (y_d - y_s) \ln a_Y + \frac{F}{RT} [z_d(E - E_d^0) - z_s(E - E_s^0)] \right\} \quad (35)$$

Equation 35 gives the activity of M_d in equilibrium with M_s .

4.2.5. Equilibrium between two solids and the aqueous phase. We next consider the equilibrium between two solids, M_u and M_v , and the aqueous phase. Equation 34 is written for each solid and equated since $(\mu_M - \mu_M^0)_u/RT = (\mu_M - \mu_M^0)_v/RT$ if the two phases are in equilibrium. The resulting equation is solved for E .

$$E = \left[\frac{z_u E_u^0 - z_v E_v^0}{z_u - z_v} \right] + \frac{(RT/F)}{(z_u - z_v)} [(x_u - x_v) \ln a_X + (y_u - y_v) \ln a_Y - 2.30259(h_u - h_v)(\text{pH})] \quad (36)$$

Equation 36 is the equation for the three phase lines that appear on Pourbaix diagrams. Substituting

Equation 36 into Equation 35 one obtains the expression for the activity of any dissolved species M_d in equilibrium with two solid phases, M_u and M_v .

$$a_d^{y_d} = \exp \left\{ \frac{1}{(z_v - z_u)} \left\{ 2.30259(\text{pH})[z_v(h_d - h_u) + z_u(h_v - h_d) + z_d(h_u - h_v)] + [z_v(x_u - x_d) + z_u(x_d - x_v) + z_d(x_v - x_u)] \ln a_X + [z_v(y_u - y_d) + z_u(y_d - y_v) + z_d(y_v - y_u)] \ln a_Y \right. \right. \\ \left. \left. + \frac{F}{RT} [z_v E_v^0(z_d - z_u) + z_u E_u^0(z_v - z_d) + z_d E_d^0(z_u - z_v)] \right\} \right\} \quad (37)$$

4.2.6. Equilibrium between three solids and an aqueous phase. When three solids and an aqueous phase co-exist at constant T and p there will be, according to Equation 8, $t = 4$ degrees of freedom. In the cases we consider here, $t = 6$, and consequently at the four-phase point there are two degrees of freedom. If the activities of X and Y are each fixed, then all other intensive thermodynamic properties are fixed, including E and pH . It is very useful to have explicit algebraic expressions for E and pH in terms of a_X and a_Y at these four-phase points. These can be obtained by writing Equation 34 for each of the three solid phases M_t , M_u and M_v . The resulting three equations are used in the equilibrium expressions to obtain two expressions between E and pH .

$$\left(\frac{\mu_M - \mu_M^0}{RT} \right)_t = \left(\frac{\mu_M - \mu_M^0}{RT} \right)_u = \left(\frac{\mu_M - \mu_M^0}{RT} \right)_v \quad (38)$$

These are, in turn, solved for E and pH . The final results, after much manipulation, are:

$$E = \left\{ z_u E_u^0(h_v - h_t) + z_v E_v^0(h_t - h_u) + z_t E_t^0(h_u - h_v) + [x_u(h_v - h_t) + x_v(h_t - h_u) + x_t(h_u - h_v)] \left(\frac{RT}{F} \right) \ln a_X + [y_u(h_v - h_t) + y_v(h_t - h_u) + y_t(h_u - h_v)] \left(\frac{RT}{F} \right) \ln a_Y \right\} A^{-1} \quad (39)$$

$$\text{pH} = - \left\{ z_u E_u^0(z_v - z_t) + z_v E_v^0(z_t - z_u) + z_t E_t^0(z_u - z_v) \right\} (F/RT) + [x_u(z_v - z_t) + x_v(z_t - z_u) + x_t(z_u - z_v)] \ln a_X + [y_u(z_v - z_t) + y_v(z_t - z_u) + y_t(z_u - z_v)] \ln a_Y \left\{ (2.30259A) \right\}^{-1} \quad (40)$$

where

$$A \equiv z_u(h_v - h_t) + z_v(h_t - h_u) + z_t(h_u - h_v) \quad (41)$$

Table 1. Solid species containing U , H and O

Species	α_i	h_i	w_i	x_i	z_i	E_i^0	Source
U	1	0	0	0	0	0	[24]
UO ₂	1	4	-2	0	4	-1.444	[24]
U ₄ O ₉	4	4.5	-2.25	0	4.5	-1.233	[24]
U ₃ O ₇ -beta	3	4.6667	-2.3333	0	4.6667	-1.172	[24]
U ₃ O ₈	3	5.3333	-2.6667	0	5.3333	-0.954	[24]
UO ₃ -gamma	1	6	-3	0	6	-0.751	[24]
UO ₃ -alpha	1	6	-3	0	6	-0.741	[24]
UO ₃ -beta	1	6	-3	0	6	-0.744	[24]
UO ₃ · H ₂ O-beta	1	6	-4	0	6	-0.771	[24]
UO ₃ · 2H ₂ O	1	6	-5	0	6	-0.769	[24]
UO ₂ (OH) ₂ -beta	1	6	-4	0	6	-0.7719	[25]
UO ₂ (OH) ₂ · H ₂ O	1	6	-5	0	6	-0.7735	[25]

4.3. Data sources

The working equations (Section 4.2) require a standard potential, E_i^0 , and a set of stoichiometric coefficients, v_i , h_i , x_i , y_i and z_i for the formation reaction for each species M_i . Tabular data used in the calculations are shown in Tables 1 through 5 for the uranium species and in Tables 6 through 8 for the chromium species.

Table 2. Dissolved species containing U, H and O

Species	α_i	h_i	w_i	x_i	z_i	E_i^0	Source
U^{3+}	1	0	0	0	3	-1.642	[24]
U^{4+}	1	0	0	0	4	-1.376	[24]
UOH^{3+}	1	1	-1	0	4	-1.483	[26]
UO_2^+	1	4	-2	0	5	-1.0125	[24]
UO_2^{2+}	1	4	-2	0	6	-0.828	[24]
$UO_2(OH)_2$	1	6	-4	0	6	-0.551	[24]
$U(OH)_2^{2+}$	1	2	-2	0	4	-1.3426	[25]
$U(OH)_3^+$	1	3	-3	0	4	-1.3039	[25]
$U(OH)_4$	1	4	-4	0	4	-1.2499	[25]
$U(OH)_5^-$	1	5	-5	0	4	-1.1819	[25]
$U_6(OH)_{15}^{3+}$	6	2.5	-2.5	0	4	-1.3336	[25]
UO_2OH^+	1	5	-3	0	6	-0.7695	[25]
$(UO_2)_2(OH)_2^{2+}$	2	5	-3	0	6	-0.7988	[25]
$(UO_2)_3(OH)_5^+$	3	5.6667	-3.6667	0	6	-0.7752	[25]

Table 3. Uranium carbonates

Species	α_i	h_i	w_i	x_i	z_i	E_i^0	Source
<i>Solid</i>							
UO_2CO_3	1	6	-3	-1	6	-0.7901	[25]
<i>Dissolved</i>							
UO_2CO_3	1	6	-3	-1	6	-0.7467	[25]
$UO_2(CO_3)_2^{2-}$	1	8	-4	-2	6	-0.6359	[25]
$UO_2(CO_3)_3^{4-}$	1	10	-5	-3	6	-0.5006	[25]

Table 4. Solid uranium fluorides

Species	α_i	h_i	w_i	x_i	z_i	E_i^0	Source
UF_3	1	0	0	-3	3	-2.063	[24]
UF_4	1	0	0	-4	4	-1.835	[24]
$UF_4 \cdot 2.5H_2O$	1	0	-2.5	-4	4	-1.889	[24]
UOF_2	1	2	-1	-2	4	-1.643	[24]
$UOF_2 \cdot H_2O$	1	2	-2	-2	4	-1.651	[24]
$UF_{4.25}$	1	0	0	-4.25	4.25	-1.660	[24]
$UF_{4.5}$	1	0	0	-4.5	4.5	-1.500	[24]
UF_5 -alpha	1	0	0	-5	5	-1.191	[24]
UF_6	1	0	0	-6	6	-0.684	[24]
$UO_2(OH)F \cdot H_2O$	1	5	-4	-1	6	-0.850	[24]
$UO_2(OH)F \cdot 2H_2O$	1	5	-5	-1	6	-0.853	[24]
UO_2F_2	1	4	-2	-2	6	-0.898	[24]

Table 5. Dissolved uranium fluorides

Species	α_i	h_i	w_i	x_i	z_i	E_i^0	Source
UF ³⁺	1	0	0	-1	4	-1.5109	[25]
UF ₂ ²⁺	1	0	0	-2	4	-1.6048	[25]
UF ₃ ⁺	1	0	0	-3	4	-1.6814	[25]
UF ₄	1	0	0	-4	4	-1.7559	[25]
UF ₅ ⁻	1	0	0	-5	4	-1.7870	[25]
UF ₆ ²⁻	1	0	0	-6	4	-1.8311	[25]
UO ₂ F ⁺	1	4	-2	-1	6	-0.8818	[25]
UO ₂ F ₂	1	4	-2	-2	6	-0.9250	[25]
UO ₂ F ₃ ⁻	1	4	-2	-3	6	-0.9536	[25]
UO ₂ F ₄ ²⁻	1	4	-2	-4	6	-0.9708	[25]

Table 6. Solid species containing Cr, H and O

Species	α_i	h_i	w_i	x_i	z_i	E_i^0	Source
Cr	1	0	0	0	0	0	[27]
Cr ₂ O ₃	2	3	-1.5	0	3	-0.611	[27]
CrO ₃	1	6	-3	0	6	+0.344	[27]
Cr(OH) ₂	1	2	-2	0	2	-0.634	[27]
Cr(OH) ₃	1	3	-3	0	3	-0.544	[27]
CrO ₂	1	4	-2	0	4	-0.169	[28]

Table 7. Dissolved species containing Cr, H and O

Species	α_i	h_i	w_i	x_i	z_i	E_i^0	Source
Cr ²⁺	1	0	0	0	2	-0.954	[27]
Cr ³⁺	1	0	0	0	3	-0.779	[27]
Cr(OH) ²⁺	1	1	-1	0	3	-0.702	[27]
Cr(OH) ₂ ⁺	1	2	-2	0	3	-0.578	[27]
Cr(OH) ₃	1	3	-3	0	3	-0.424	[27]
Cr ₂ (OH) ₂ ⁴⁺	2	1	-1	0	3	-0.729	[27]
Cr ₃ (OH) ₄ ⁵⁺	3	1.333	-1.333	0	3	-0.725	[27]
Cr(OH) ₄ ⁻	1	4	-4	0	3	-0.239	[27]
CrO ₂ ⁻	1	4	-2	0	3	-0.228	[27]
CrO ₂ ²⁻	1	8	-4	0	6	0.375	[27]
HCrO ₄ ⁻	1	7	-4	0	6	0.311	[27]
H ₂ CrO ₄	1	6	-4	0	6	0.32	[27]
Cr ₂ O ₇ ²⁻	2	7	-3.5	0	6	0.304	[27]
CrO ₃ ³⁻	1	6	-3	0	3	0.374	[28]
CrO ₄ ³⁻	1	8	-4	0	5	0.438	[29]

The data were obtained from standard secondary sources listed in the tables. Standard potentials, E_i^0 , were computed from standard free energies of formation using Equation 25 with $\mu_n^0 = \Delta G_{f,n}^0$. The data sets are believed to include all important species. However, obviously no guarantee can ever be made that a data set is, in fact, complete.

It is interesting that in both of these relatively complex systems, no species were found in which six primitive species were required, i.e. no uranium species involving both F⁻ and CO₂ and no chromium species involving both Cl⁻ and CO₂.

Table 8. Chromium chlorides

Species	α_i	h_i	w_i	x_i	z_i	E_i^0	Source
<i>Solid</i>							
CrCl ₂	1	0	0	-2	2	-0.484	[27]
CrCl ₃	1	0	0	-3	3	-0.311	[27]
<i>Dissolved</i>							
CrCl ₂ ⁺	1	0	0	-2	3	-0.748	[27]
CrCl ₂ ²⁺	1	0	0	-1	3	-0.762	[27]
CrOHCl ₂	1	1	-1	-2	3	-0.636	[27]
CrO ₃ Cl ⁻	1	6	-3	-1	6	+0.303	[27]

5. Construction of Pourbaix diagrams

5.1. Structure of Pourbaix diagrams

When a_x and a_y are fixed, the Pourbaix diagram is a three-dimensional surface which divides the E , pH and $\log a_M$ space into a region where a single aqueous phase exists, and an inaccessible region beyond the solubility limit. The surface is comprised of one or more curved surfaces where a single solid is in equilibrium with the aqueous phase. These surfaces intersect to form curvilinear lines along which three phases (two solids plus the aqueous phase) coexist. There are places where three surfaces come together at four-phase (three solids plus the aqueous phase) points. Each four-phase point is connected to three other four-phase points by three-phase lines. Connected four-phase points share a common pair of solids.

A projection of the three-dimensional figure onto the E -pH plane is normally reported. On this projection the three-phase lines and the contours of constant activity, a_M , are plotted.

When the solids are of constant composition, the three-phase lines are straight lines in the two dimensional E -pH projection. This may easily be seen from Equation 36. The slope of Equation 36 is $-2.30259(h_u - h_v)RT/F(z_u - z_v)$. For systems containing only the elements M, H and O, one has $h_s = z_s$ for uncharged solid phases and consequently the slope is the same for all three-phase lines. In general, for more complex systems with additional elements, $h_s \neq z_s$, and therefore the slopes of the various three-phase lines are not the same.

5.2. Computation of four-phase points

One first considers each possible triple, M_t , M_u , M_v , of solids. The E and pH of each possible four-phase point are computed using Equations 39, 40 and 41. At this value of E and pH the value of $(\mu_M - \mu_M^0)_{t,u,v}/RT$ is calculated using Equation 34. Then $(\mu_M - \mu_M^0)_s/RT$ is computed for all other solid phases. If $(\mu_M - \mu_M^0)_{t,u,v}/RT < (\mu_M - \mu_M^0)_s/RT$ for all other solids (M_s) then this four-phase point is stable. Furthermore, if the values of E and pH are within the range plotted, e.g. $-3 \text{ V} < E < +3 \text{ V}$ and $-2 < \text{pH} < 16$, the point will appear on the E -pH diagram.

The number of computations at this stage of the calculation can be formidable. The total number of triples of solids, n_T , that can be chosen from n_s solids is:

$$n_T = \frac{n_s!}{(n_s - 3)!3!} \quad (42)$$

The number of possible solids can be 20 or more for complex systems. For $n_s = 20$, one has a total of 1140 triples that must be individually considered.

5.3. Determination of three-phase lines

After the (E , pH) coordinates of all stable four-phase points are calculated and saved, the points are tested to see how they are connected with one another. Two four-phase points are connected by a three-phase line if the points share two common solid phases. The four-phase points can all be placed in three categories: (i) points within the E , pH range of the diagram that are connected only to other points also within the range; (ii) points within the E , pH range of the diagram which are connected to one or two points without the range; and (iii) points without the range that are connected to other points without the range.

Points in the first category can be connected by the plotting routine without further consideration. Points in the second and third categories can be connected with points on the lines defining the boundary of the diagram, e.g. $E = -3\text{ V}$, $E = +3\text{ V}$, $\text{pH} = 0$ and $\text{pH} = 14$. The E and pH values of the intersections of the three-phase lines (Equation 36) with these boundary values are computed. The intersection is kept if it falls within the range of the diagram and if it meets the stability criterion, i.e. if $(\mu_M - \mu_M^0)/RT$ for this solid pair is less than that for every other solid phase. The diagram is completed by drawing straight lines between surviving intersections which share a common pair of solids.

5.4. Computation of contours of constant activity or concentration

In addition to the network of three-phase lines, contours of constant activity, a_M , of the active redox element can be projected onto the E -pH plane. The activity is defined as in [17]:

$$a_M = \sum a_d^{v_d} \quad (43)$$

where the sum is taken over all dissolved species. Equation 43 is used together with Equation 37 to give the total activity at any point along one of the three-phase lines. The desired value of a_M is chosen, e.g. 0.1, and the bisection method used to determine the points, if any, along the three-phase line and the boundary lines where this value exists. These points are used as the starting points for a routine that traces out the contours of constant a_M in the two-phase (solid plus aqueous) regions. Equations 43 and 35 are used with Newton's damped method to trace out the contours. These contours are not, in general, straight lines.

If activity coefficients are known, or can be assumed to be unity, the contours of constant concentration of active element can be traced out. In this event one uses the definition of the total concentration

$$[M]_T = \sum \alpha_d [M_d] \quad (44)$$

together with Equations 35 and the relation $a_i = \gamma_i [M_i]$. Since $a_i^{v_i} = (\gamma_i [M_i])^{v_i}$ and $\alpha_i \equiv 1/v_i$, Equations 43 and 44 are identical only when $\gamma_i = 1$ and $v_i = 1$ for all dissolved species.

6. Construction of predominance diagrams

The network of lines that divides the E -pH field into regions of dominance of individual dissolved species is determined by the criterion

$$a_b^{v_b} = a_c^{v_c} \quad (45)$$

Using Equation 32 in Equation 45 one finds the relationship between E and pH for any arbitrary dissolved pair:

$$E = \left[\frac{z_b E_b^0 - z_c E_c^0}{z_b - z_c} \right] + \frac{(RT/F)}{z_b - z_c} [(x_b - x_c) \ln a_x + (y_b - y_c) \ln a_y - 2.30259(h_b - h_c) \text{pH}] \quad (46)$$

It is important to note that Equation 46 is independent of the concentration of the active element.

Except for the different interpretation of the indices, Equation 46 is identical to Equation 36. Therefore, Equations 39 and 40 can be used to determine E and pH where three dissolved species have identical values of a_i^v .

The algorithm for constructing the predominance diagrams is almost identical to that for constructing the network of three-phase lines on Pourbaix diagrams. The only difference is the use of a different criterion to discard points. When constructing a predominance diagram, a three-species point (where $a_b^{v_b} = a_c^{v_c} = a_d^{v_d}$) is kept only if $a_b^{v_b}$ is greater than $a_n^{v_n}$ for all other dissolved species, M_n .

When the procedure is completed, the E -pH field is divided into regions which show the dominance of individual ions. The boundaries between the regions are given by the condition of Equation 45 and the equations of the straight lines joining the points are given by Equation 46.

7. Examples of diagrams

7.1. Uranium and chromium Pourbaix diagrams

The program was implemented in BASIC on an IBM-PC/AT personal computer. Hard copies of the diagrams were obtained with either a dot matrix printer or a plotter.

An example of a diagram for the U-H-O system is shown in Fig. 1. The three-phase lines are parallel as expected. The program automatically prints the code number for the stable solid phase at the value of E and pH given by the arithmetic average of the values at the vertices of the stability field for that solid. Constant activity lines are shown as light dashed lines at values of a_U of 1, 10^{-5} and 10^{-8} .

A very different diagram is obtained when F^- ion is maintained at an activity of $a_{F^-} = 10^{-4}$. This diagram is shown in Fig. 2. A number of solids containing fluorine are stable and the contours of constant uranium activity have been significantly altered. Because this is a four-element system, i.e. U, O, H and F, the three-phase lines are no longer always parallel. Increasing the F^- concentration does not change the solids present, but does shift the stability fields and the contours of constant uranium activity.

Addition of CO_2 to the system at an activity of $a_{CO_2} = 3.3 \times 10^{-4}$ changes the activity contours slightly but the solids remain unchanged (Fig. 3). (The activity of CO_2 in air at atmospheric pressure

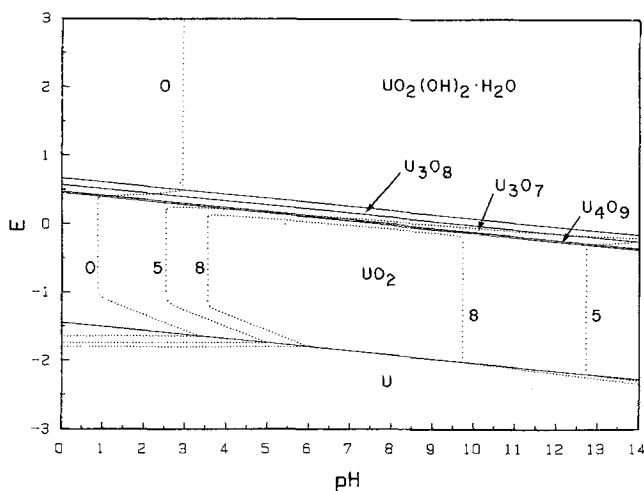


Fig. 1. Pourbaix diagram for the U-H-O system. Constant uranium activity contours at $a_U = 1$, 10^{-5} and 10^{-8} are shown as dotted lines (0, 5 and 8, respectively).

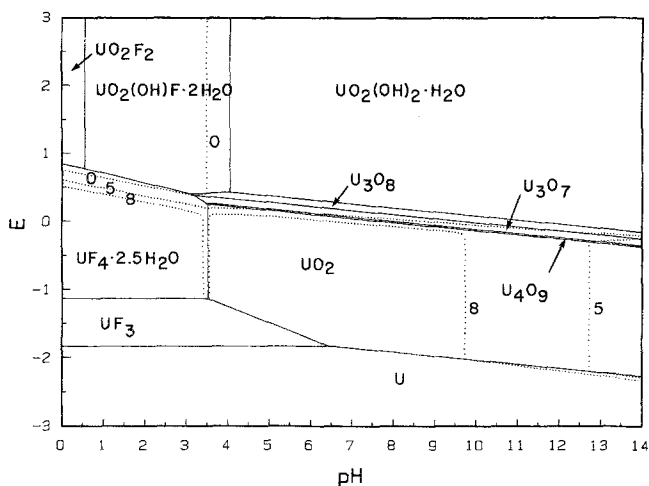


Fig. 2. Pourbaix diagram for the U-H-O-F system. Fluoride ion activity fixed at $a_{F^-} = 10^{-4}$. Constant uranium activity contours at $a_U = 1, 10^{-5}$ and 10^{-8} are shown as dotted lines (0, 5 and 8, respectively).

is approximately 3.3×10^{-4} .) The Pourbaix diagram when both F^- and CO_2 are present is shown in Fig. 4.

The Pourbaix diagram for the chromium system (Cr-H-O) is shown in Fig. 5. The three-phase lines are parallel. Contours of constant activity are shown at $a_{Cr} = 1, 10^{-4}$ and 10^{-8} . The Pourbaix diagrams for the Cr-H-O-Cl system with $a_{Cl^-} = 0.1$ and $a_{Cl^-} = 1$ were also computed. Within the error of the plotter, these diagrams are identical to Fig. 5. These results indicate either that Cl^- ions do not influence the equilibrium phase chemistry in this system or that important species containing these elements were not included in the data base used.

7.2. Uranium and chromium predominance diagram

The predominance diagram for the uranium system (U-H-O) system is shown in Fig. 6. Addition of F^- ion at an activity of $a_{F^-} = 10^{-4}$ greatly changes the dominant ions. Two complex species containing fluorine, UF_4 and UO_2F_2 , now appear among the dominant dissolved species, replacing UO_2^{2+} and $(UO_2)_2(OH)_2^{2+}$ (see Fig. 7). Increasing a_{F^-} further alters the diagram in the direction of greater stability of the fluoride complex ions as expected.

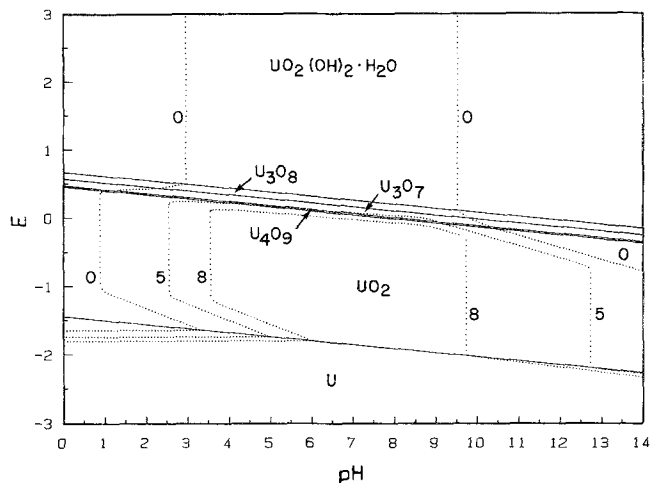


Fig. 3. Pourbaix diagram for the U-H-O-C system. Carbon dioxide activity fixed at $a_{CO_2} = 3.3 \times 10^{-4}$. Constant uranium activity contours at $a_U = 1, 10^{-5}$ and 10^{-8} are shown as dotted lines (0, 5 and 8, respectively). Carbonates were the only carbon-containing species used in data base for this diagram.

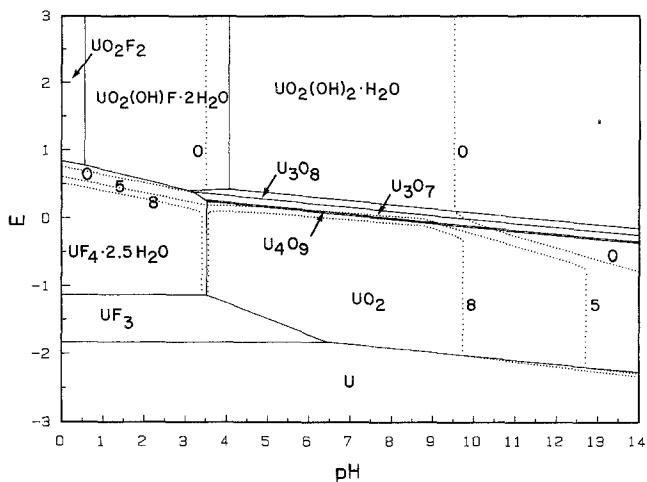


Fig. 4. Pourbaix diagram for the U-H-O-F-C system. Fluoride ion activity fixed at $a_{\text{CO}_2} = 3.3 \times 10^{-4}$. Constant uranium activity contours at $a_{\text{U}} = 1, 10^{-5}$ and 10^{-8} are shown as dotted lines (0, 5 and 8, respectively). Carbonates were the only carbon-containing species used in data base for this diagram.

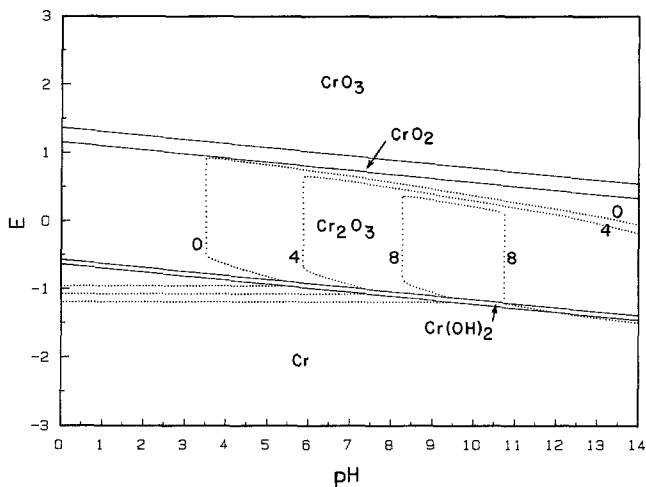


Fig. 5. Pourbaix diagram for the Cr-H-O system. Constant chromium activity contours at $a_{\text{Cr}} = 1, 10^{-4}$ and 10^{-8} are shown as dotted lines (0, 5 and 8, respectively).

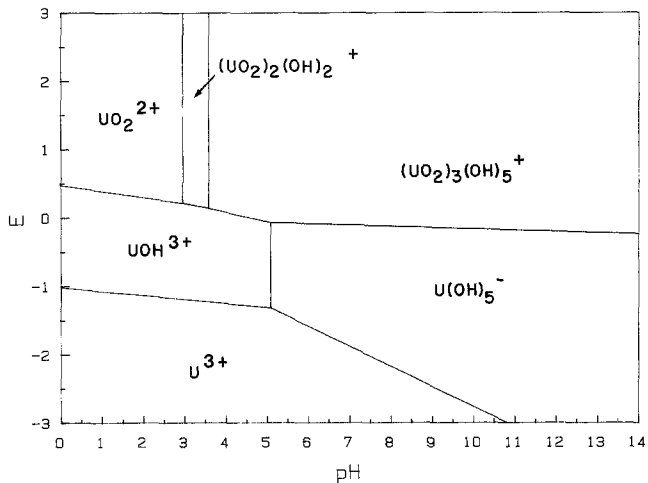


Fig. 6. Predominance diagram for the U-H-O system.

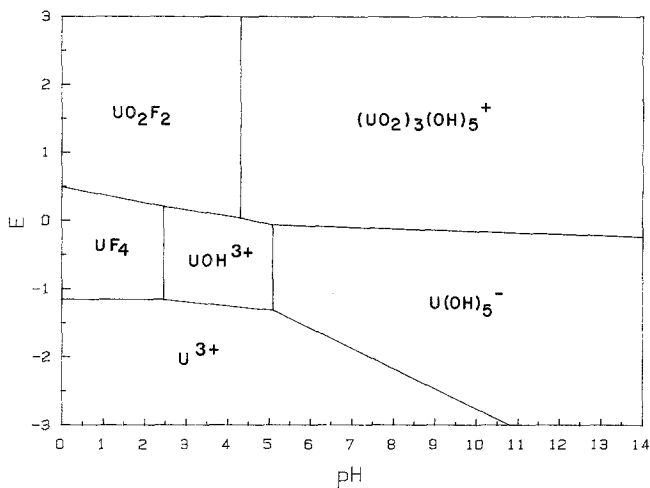


Fig. 7. Predominance diagram for the U-H-O-F system. Fluoride ion activity fixed at $a_{F^-} = 10^{-4}$.

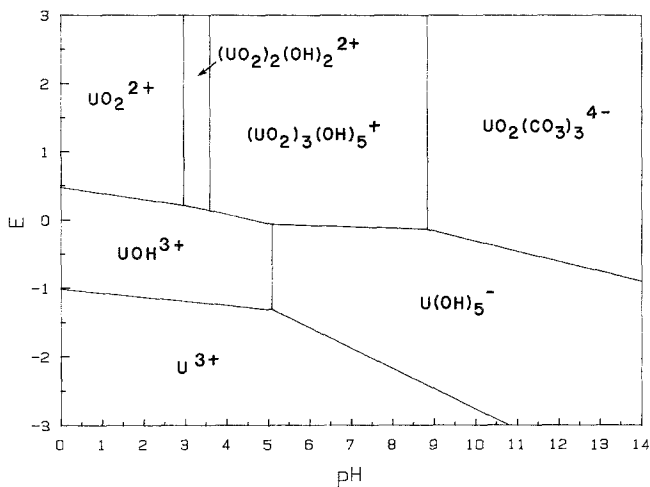


Fig. 8. Predominance diagram for the U-H-O-C system. Carbon dioxide activity fixed at $a_{CO_2} = 3.3 \times 10^{-4}$. Carbonates were the only carbon-containing species used in data base for this diagram.

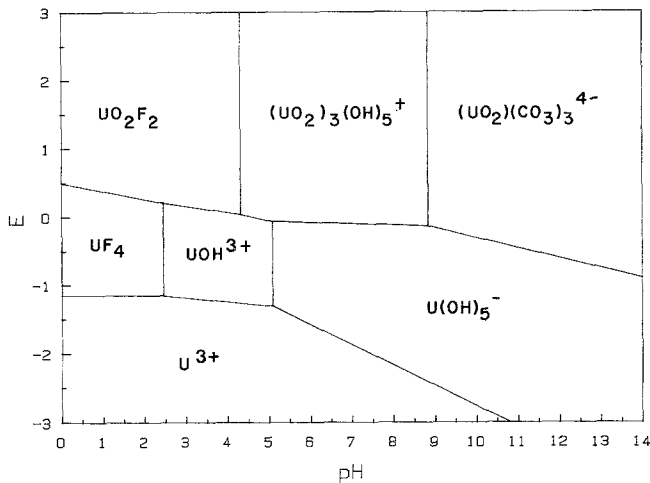


Fig. 9. Predominance diagram for U-H-O-F-C system. Fluoride ion activity fixed at $a_{F^-} = 10^{-4}$. Carbon dioxide activity fixed at 3.3×10^{-4} . Carbonates were the only carbon-containing species used in data base for this diagram.

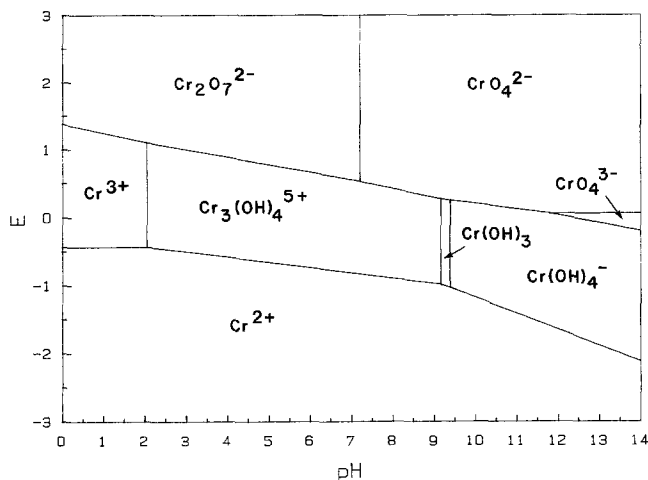


Fig. 10. Predominance diagram for the Cr-H-O system.

When CO_2 is added to the system at an activity of $a_{\text{CO}_2} = 3.3 \times 10^{-4}$, the predominance diagram is significantly changed. The carbonate complex ion $\text{UO}_2(\text{CO}_3)_3^{4-}$ becomes dominant at high potential and pH (compare Figs 6 and 8). A predominance diagram for the uranium system with both $a_{\text{F}^-} = 10^{-4}$ and $a_{\text{CO}_2} = 3.3 \times 10^{-4}$ is shown in Fig. 9.

The predominance diagram for chromium (Cr-H-O) is shown in Fig. 10. The predominance diagram for the Cr-H-O-Cl system at $a_{\text{Cl}^-} = 0.01$ is identical to that when Cl^- is absent. If the activity of Cl^- is increased to $a_{\text{Cl}^-} = 1.0$, the CrO_3Cl^- ion becomes dominant only at $\text{pH} < 0.1$ and $E > 1.4$. These results are consistent with the lack of influence of the activity of Cl^- on the calculated Pourbaix diagrams.

8. Discussion

8.1. Pourbaix diagrams and predominance diagrams

Potential-pH diagrams which show the stability fields of the solids and the contours of a_M are called Pourbaix diagrams; potential-pH diagrams which show the regions of dominance of dissolved species have been called predominance diagrams. The two diagrams are often superimposed to show the dominant dissolved species in each part of the solid stability field [2, 3].

It is important to keep the distinction between the two types of diagrams clear. In some studies a 'hybrid' type of predominance diagram of dissolved and solid species has been presented. A Pourbaix diagram is most useful when the stability fields of the solids are calculated using *all* dissolved species. On the other hand, a predominance diagram is most useful when it contains *only* dissolved species and, moreover, when the diagram is constructed in such a way as to be independent of concentration [17].

It must be emphasized that the 'hybrid' potential-pH diagrams can not show true solid-aqueous phase boundaries (contours of constant a_M) because non-major dissolved species are excluded when determining the boundaries. The solid-aqueous boundaries are, in general, curved lines and do not form a polygonal structure in the E -pH field. Only in the special cases where the concentration of the dominant ion is very much greater than the concentration of all other ions are the solid-aqueous boundaries straight lines.

The procedure recommended here gives diagrams which are more closely related to experimentally determined diagrams and, moreover, is consistent with the original conception of Pourbaix [1].

8.2. Computational method and equation balancing

After choosing the primitive species and entering the stoichiometric coefficients and standard potentials for the formation reactions, no further balancing of chemical reactions is required. Furthermore, there is no distinction between reactions involving a redox transition of M and those that do not; all reactions are written as formation reactions from the primitive species. One great advantage of this procedure is that species can be eliminated or added at will to the data set without changing the algebraic structure of the problem.

Furthermore, it can be noted from Equation 32 that the activities, a_i , of all species can be solved sequentially rather than simultaneously if the activities of the primitive species are known. This provides great computational simplification. However, if the concentrations of the dissolved species, $[M_i]$, are desired, then a simultaneous solution of the equations must be performed. This is because the concentrations are related to the activities through the relation $[M_i] = a_i/\gamma_i$, where γ_i is, in general, a function of the concentrations of all other species.

8.3. Mole balance and atom balance constraints

The computational methods described here are extremely efficient for situations where the equilibrium state is defined by imposed constraints of constant chemical potential; for example, when CO_2 activity is fixed. There are situations, however, when the equilibrium state is defined by a mole or atom balance constraint. Often the total moles of related dissolved species, e.g. H_2CO_3 , HCO_3^- and CO_3^{2-} are constant; a case of this type involving dissolved H_2S , HS^- and S^{2-} has been described by McDonald and Syrett [23]. The general methods described here, with slight extension, can be applied to these situations.

One method to achieve a mole balance on related dissolved species, e.g. CO_3^{2-} , HCO_3^- and H_2CO_3 , is to perform an iterative calculation. The activity of the appropriate primitive species, e.g. CO_2 , would be varied until the total concentration, $[C] \equiv [\text{CO}_3^{2-}] + [\text{HCO}_3^-] + [\text{H}_2\text{CO}_3]$, reached the desired value. In the more general case the dissolved species may form other complexes and this must be taken into account. For example, for the uranium system the total carbonate concentration will be given by $[C] \equiv [\text{CO}_3^{2-}] + [\text{HCO}_3^-] + [\text{H}_2\text{CO}_3] + [\text{UO}_2(\text{CO}_3)] + 2[\text{UO}_2(\text{CO}_3)_2^{2-}] + 3[\text{UO}_2(\text{CO}_3)_3^{4-}]$.

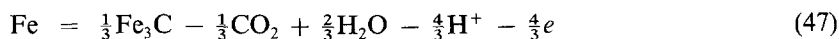
Another option is to derive the specific equilibrium relationship between the activity of the primitive species, e.g. a_{CO_2} , and the total concentration, $[C]$, of related species. This expression can be used to replace a_x in the equations which define the potential-pH diagram. Diagrams drawn in this manner would describe the situation where $[C]$ was held constant. Since the details of this approach are specific to the particular application, they are not further described.

Improper choice of constraints can lead to calculated diagrams which are wildly unrealistic. For example, using CO_3^{2-} as a primitive species at low pH and fixing $a_{\text{CO}_3^{2-}} = 1$ would imply enormous CO_2 pressures. Similar effects can be present when dealing with ions that are strongly complexed, e.g. Cl^- ions in copper solutions. In this case a constraint of total chlorine concentration might be more appropriate than a constraint of fixed activity of Cl^- . In all cases it is essential that the calculations be performed while keeping in mind the chemistry of the system.

8.4. Additional redox elements

The computational method automatically allows the incorporation of other elements which may undergo redox transitions. For example, consider the Fe system in the presence of H_2O and gaseous CO_2 . If the data base for the solid iron compounds includes iron carbide as well as the solid carbonates and oxides, the methods will produce a diagram in which the stable carbide phases, if

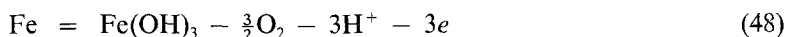
any, are shown. The standard formation reaction in this case would be



(Carbide phases were not included in the data based used to generate Figs 1 through 5.)

This procedure provides great flexibility and generality in developing potential–pH diagrams for specific applications. For example, in hydrometallurgical processes it might be useful to develop diagrams in which the partial pressure of H_2S is controlled.

One can also develop diagrams in which O_2 replaces H_2O as the primitive species supplying oxygen. Consider for example, the standard reactions for $\text{Fe}(\text{OH})_3$.



Equations analogous to Equation 48 would be useful in describing situations where the oxygen partial pressure and the pH were controlled. In both Equations 47 and 48 note that z_i , the stoichiometric coefficient for the electrons, no longer has the simple interpretation as the electrochemical valence of iron in Fe_3C or $\text{Fe}(\text{OH})_3$. This is simply because other elements (C and O) are also changing their oxidation state.

The chemical potential of the additional redox elements, e.g. C and O in the above examples, is fixed by fixing the chemical potentials of the primitive species in question. The chemical potential of the primary redox element, Fe in the above examples, is allowed to vary. One could contemplate diagrams in which the chemical potentials of both redox species were allowed to vary. In order to reduce the corresponding diagram to two dimensions it would be necessary to fix one other chemical potential, most likely the pH.

Acknowledgements

The authors wish to acknowledge the support of Martin Marietta Energy Systems (Oak Ridge) under contract to the Department of Energy and the support of the US Army Research Office.

References

- [1] M. Pourbaix, 'Thermodynamics of Dilute Aqueous Solutions: Graphical Representation of the Role of pH and Potential', Thesis, Delft (1945); CEBELCOR Publication F. 227 (reprinted in 1963 in French).
- [2] *Idem*, 'Atlas of Electrochemical Equilibria in Aqueous Solutions', Pergamon Press, New York and CEBELOR, Brussels (1966).
- [3] *Idem*, 'Lectures on Electrochemical Corrosion', Plenum Press, New York (1973).
- [4] M. Pourbaix and A. Pourbaix (eds), 'Diagrams of Chemical and Electrochemical Equilibria: Their Setting-Up and Applications', Proceedings of a NATO Advanced Research Workshop, Brussels, 2–5 September, 1981, CEBELCOR's Reports Techniques **142**, RT 263, CEBELOR, Brussels (1982).
- [5] P. A. Brook, *Corrosion Sci.* **11** (1971) 389.
- [6] D. D. MacDonald, G. R. Shierman and P. Butler, 'The Thermodynamics of Metal–Water Systems at Elevated Temperatures. Part I: The Water and Copper–Water Systems', Atomic Energy of Canada, Chalk River, Ontario AECL-4136 (1972) p. 91.
- [7] L. Santoma, *Bol. Geol. Miner.* **84** (1973) 156.
- [8] M. H. Froning, M. E. Shanley and E. D. Verink, Jr, *Corrosion Sci.* **16** (1976) 371.
- [9] J. S. Newton and P. F. Duby, *Nucl. Metall.* **20** (1976) 951.
- [10] B. G. William and W. J. Patrick, *J. Chem. Educ.* **54** (1977) 107.
- [11] A. D. Pelton, C. W. Bale and W. I. Thompson, Nat. Bureau of Standards SP-496, 'Applications of Phase Diagrams in Metallurgy and Ceramics', Proceedings of Workshop held at Gaithersburg, MD, 10–12 January, 1977, p. 1077.
- [12] B. H. Rosof, *ibid.*, p. 1090.
- [13] P. B. Linkson, B. E. Phillips and C. D. Rowles, *Miner. Sci. Eng.* **11** (1979) 65.
- [14] B. C. Syrett, D. D. MacDonald and H. Shih, *Corrosion* **36** (1980) 130.
- [15] T. I. Barry, in 'Thermodynamics of Aqueous Systems with Industrial Applications', ACS Symposium Series 133 (edited by S. A. Newman) ACS, Washington, DC (1980) p. 681.
- [16] C. M. Chen and K. Aral, *Corrosion* **38** (1982) 183.
- [17] J. C. Angus and C. T. Angus, *J. Electrochem. Soc.* **132** (1985) 1014.
- [18] S. R. Brinkley, Jr, *J. Chem. Phys.* **15** (1947) 107.

- [19] K. Denbigh, 'The Principles of Chemical Equilibrium', 4th edn, Cambridge University Press, Cambridge (1981).
- [20] W. B. White, *J. Chem. Phys.* **46** (1967) 4171.
- [21] J. B. Ramsey, *J. Electrochem. Soc.* **104** (1957) 255.
- [22] G. N. Lewis, M. Randall, K. S. Pitzer and L. Brewer, 'Thermodynamics', McGraw Hill, New York (1961).
- [23] D. D. MacDonald and B. C. Syrett, *Corrosion* **35** (1979) 471.
- [24] D. D. Wagman, W. H. Evans, V. P. Parker, R. H. Schumm, I. Halow, S. M. Bailey, K. L. Churney and R. L. Nuttal, 'The NBS Tables of Chemical Thermodynamic Properties: Selected Values for Inorganic and C₁ and C₂ Organic Substances in S.I. Units', National Bureau of Standards, Washington, DC (1982).
- [25] D. Langmuir, *Geochimica* **42** (1978) 547.
- [26] H. E. Barner and R. V. Scheuerman, 'Handbook of Thermodynamical Data for Compounds and Aqueous Species', Wiley Interscience, New York (1978).
- [27] R. L. Schmidt, 'Thermodynamic Properties and Environmental Chemistry of Chromium', US DOE Contract DC-AC06-76RLO 1830, July 1984.
- [28] P. Radhakrishnamurty and P. Adaikkalam, *Corros. Sci.* **22** (1982) 753.
- [29] I. Dellien, F. M. Hall and L. G. Hepler, *Chem. Rev.* **76** (1976) 283.